ORGANIC LETTERS

2012
Vol. 14, No. 23
5836–5839

Quantum Mechanical Transition-State Analysis Reveals the Precise Origin of Stereoselectivity in Chiral Quaternary Cinchonidinium Phase-Transfer Catalyzed Enolate Allylation

Thomas C. Cook, Merritt B. Andrus,* and Daniel H. Ess*

Department of Chemistry and Biochemistry, Brigham Young University, Provo, Utah, 84602, United States

dhe@chem.byu.edu; mbandrus@chem.byu.edu

Received September 26, 2012

ABSTRACT

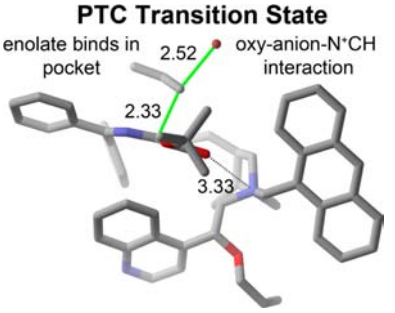

Density functional theory was used to model glycinate enolate binding and enantiomeric allylation transition states mediated by the cinchonidinium phase-transfer catalyst 2. Transition states show oxy-anion-ammonium interactions in contrast to π-face interactions in the ground states. The details of stereoselectivity are described within the quaternary ammonium-tetrahedron face model.

Ion-pairing catalysis has become a popular paradigm for asymmetric organic transformations.[1] Phase-transfer[2] type ion-pairing catalysis has proven especially useful for asymmetric enolate alkylation and allylation.[3] Initial work by Dolling[4] and separately by O'Donnell[5] using Schiff base glycine showcased the potential and versatility of using cinchona-alkaloid-derived chiral quaternary ammonium salts as phase-transfer catalysts. Cinchona alkaloids are also advantageous because they are readily available at a low cost, are easily derivatized, and provide catalysis under relatively mild conditions.[6]

In 1997 Corey et al.[7] disclosed the highly enantioselective glycine alkylation/allylation reaction catalyzed by the cinchonidinium (CD) 9-methylanthracenyl phase-transfer catalyst **2** (Scheme 1). Separately Lygo and Wainwright reported a similar catalyst also with high enantioselectivity.[8] The Corey design was based on considering the bridgehead nitrogen of the cinchona quaternary salt as a tetrahedron (Scheme 2a) where three of the four faces are sterically screened by the alkaloid quinuclidine structure, 9-anthracenyl group, and O-allyl group. Catalyst **2** exhibited between 92% and >99% enantioselectivity for the *S*-alkylation and allylation products (**3**) of the O'Donnell

(1) Phipps, R. J.; Hamilton, G. L.; Toste, F. D. *Nat. Chem.* **2012**, *4*, 603.
(2) Starks, C. M. *J. Am. Chem. Soc.* **1971**, *93*, 195.
(3) (a) Maruoka, K.; Ooi, T. *Chem. Rev.* **2003**, *103*, 3013. (b) O'Donnell, M. J. *Acc. Chem. Res.* **2004**, *37*, 506. (c) Lygo, B.; Andrews, B. I. *Acc. Chem. Res.* **2004**, *37*, 518. (d) Ooi, T.; Maruoka, K. *Angew. Chem., Int. Ed.* **2007**, *46*, 4222. (e) Hashimoto, T.; Maruoka, K. *Chem. Rev.* **2007**, *107*, 5656. (f) Maruoka, K., Ed. *Asymmetric Phase Transfer Catalysis*; Wiley-VCH: Verlag GmbH & Co.: 2008.
(4) Dolling, U. H.; Davis, P.; Grabowski, E. J. J. *J. Am. Chem. Soc.* **1984**, *106*, 446.
(5) (a) O'Donnell, M. J.; Bennett, W. D.; Wu, S. *J. Am. Chem. Soc.* **1989**, *111*, 2353. (b) O'Donnell, M. J.; Wu, S.; Huffman, J. C. *Tetrahedron* **1994**, *50*, 4507.
(6) Kacprzak, K.; Gawronski, J. *Synthesis* **2001**, 961.
(7) Corey, E. J.; Xu, F.; Noe, M. C. *J. Am. Chem. Soc.* **1997**, *119*, 12414.
(8) Lygo, B.; Wainwright, P. G. *Tetrahedron Lett.* **1997**, *38*, 8595.

10.1021/ol3026582
Published on Web 11/19/2012

Scheme 1. Example of General Conditions for Alkylation/Allylation of the O'Donnell Schiff Base by Catalyst CN **2**

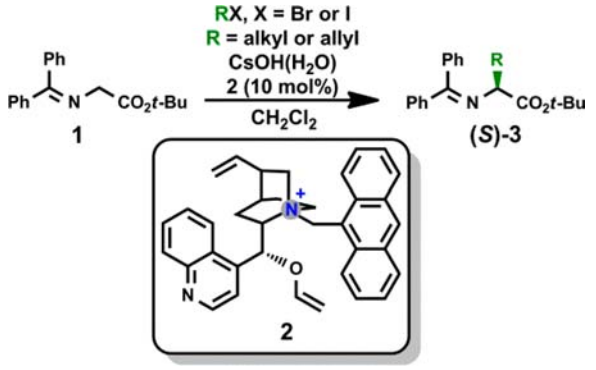

tert-butyl glycinate-benzophenone Schiff base **1** (Scheme 1).[7] Catalyst **2** was also compatible with a wide range of electrophilic RX partners, including alkyl iodides, benzyl bromides, and allyl bromides.[7] High enantioselectivity was also reported by Corey and co-workers for CD catalyst **2** for alkylation and allylation of similar dieneolates.[9] In general, use of the pseudoenantiomeric cinchonine (CN) derived catalyst, with C8 and C9 inverted and the vinyl stereochemistry maintained, allows for generation of the corresponding **(*R*)-3** products.

While phase-transfer catalysis has achieved notable success with some substrates, there remains a lack of details concerning the origin of enantioselectivity, mode of enolate binding, and identification of design principles that govern complementary pro-*R* and pro-*S* substrate–catalyst electophile interactions. Computational investigation of PTC reactions has been limited due to the large size of the catalysts and the need to accurately treat weak van der Waals and London dispersion-type interactions. Notable is the work of Cannizzaro and Houk[10] who used MP2 calculations to explore the interaction of enolates with a $(CH_3)_3NH^+$ quaternary ammonium model. They found that the most stable enolate–$(CH_3)_3NH^+$ complex involved interaction between the π-face of the enolate and the ammonium cation through N^+-C-H π-interactions (Figure 2b). This suggests that asymmetric induction is the result of complete facial blocking of one of the two enolate π-faces. Based on molecular mechanics and semiempirical methods Lipkowitz and O'Donnell have also suggested that stereoselectivity is a result of π-facial interaction between the enolate and quaternary ammonium.[11]

Here we report density functional calculations that examine the enantiomeric transition states for allylation of the enolate derived from Schiff base **1** catalyzed

Scheme 2. Models of Asymmetric Stereoselectivity

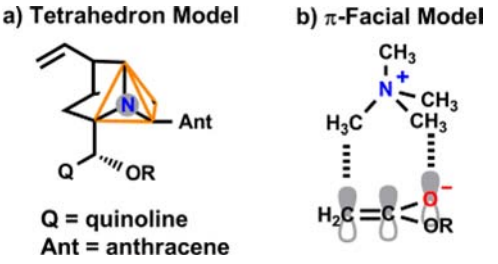

by CD **2**. Structures were optimized with the M06-2X[12] functional using an ultrafine integration grid in *GAUSSIAN 09*.[13] The 6-31G(d,p) basis set was used for all atoms except Br where LANL2DZ was used. The larger 6-311+G(2d,p)[LANL2TZ(f) for Br] basis set was also used to evaluate energies but in general showed less than 0.2 kcal/mol energy differences. The M06-2X method was chosen since it accurately reproduces weak interaction energies, such as CH–π and $\pi-\pi$ interactions.[12,14] Minima and transition structures were confirmed by calculation of the Hessian and vibrational normal mode inspection. Dichloromethane solvent effects were estimated using the SMD model.[15] The ΔE_{soln} values reported are the sum of ΔE and ΔG_{sol} values.

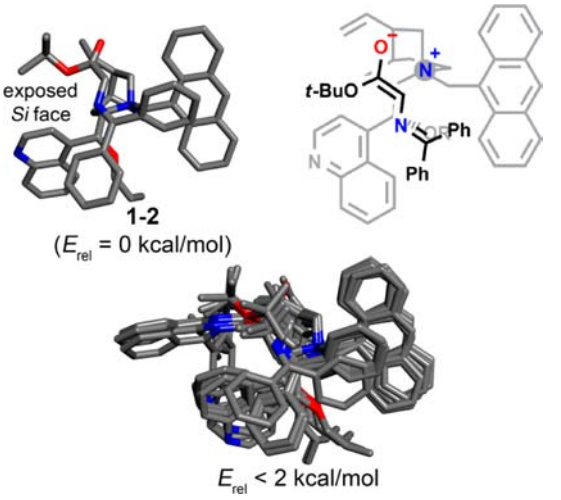

Figure 1. Top: lowest energy enolate–catalyst complex (**1**–**2**). Bottom: RMSD ensemble overlay of the 10 lowest energy complexes. Hydrogen atoms were removed for clarity.

Initially we explored the ground-state coordination complexes of catalyst **2** with enolate (*E*)-**1**.[16] A search of ground-state structures was done systematically with

(9) Corey, E. J.; Bo, Y.; Busch-Petersen, J. *J. Am. Chem. Soc.* **1998**, *120*, 13000.
(10) Cannizzaro, C. E.; Houk, K. N. *J. Am. Chem. Soc.* **2002**, *124*, 7163.
(11) Lipkowitz, K. B.; Cavanaugh, M. W.; Baker, B.; O'Donnell, M . J. *J. Org. Chem.* **1991**, *56*, 5181.
(12) (a) Zhao, Y.; Truhlar, D. G. *Theor. Chem. Acc.* **2008**, *120*, 215. (b) Zhao, Y.; Truhlar, D. G. *Acc. Chem. Res.* **2008**, *41*, 157.
(13) Frisch, M. J.; et al. *Gaussian 09*, revision A.02; Gaussian, Inc.: Wallingford, CT, 2009.
(14) Grimme, S. *WIREs Comput. Mol. Sci.* **2011**, *1*, 211.
(15) Marenich, A. V.; Cramer, C. J.; Truhlar, D. G. *J. Phys. Chem. B* **2009**, *113*, 6378.
(16) Here we report the analysis for allylation of only enolate (*E*)-**1**. This enoloate was proposed in Corey's model (ref 9). See the Supporting Information discussion of transition states for enolate (*Z*)-**1**.

π-facial and oxy-anion (π-face perpendicular) approaches of the enolate to the three open faces of catalyst **2** with consideration of all possible conformations of the enolate and the catalyst quinoline, anthracenyl, allyl, and O-allyl groups. This search led to an ensemble of several hundred unique structures. In accordance with the previous work by Cannizzaro and Houk[9] the lowest energy (*E*)-**1**−catalyst **2** complex (**1**−**2**) showcases an enolate that interacts with **2** via flat-π-facial interactions (Figure 1). In **1**−**2** the CO_2t-Bu group protrudes on top of the allyl group of the bicyclic ring structure while the enolate phenyl groups are oriented to interact with both the anthracenyl and quinoline groups. Although **1**−**2** is lowest in energy this complex exposes the incorrect π-face (*Si*) and would lead to **(*R*)-3** and not **(*S*)-3**. However, **1**−**2** is only one of several low energy enolate−catalyst complexes. Figure 1 shows an overlay of the 10 lowest energy enolate−catalyst complexes that differ in energy by less than 2 kcal/mol compared to **1**−**2**. Within this set of complexes there are only two major binding modes that the enolate interacts with **2**. The first is similar to **1**−**2** while the second mode involves exposure of the *Re* enolate face by flipping the orientation of the enolate while remaining in a roughly similar binding pocket.

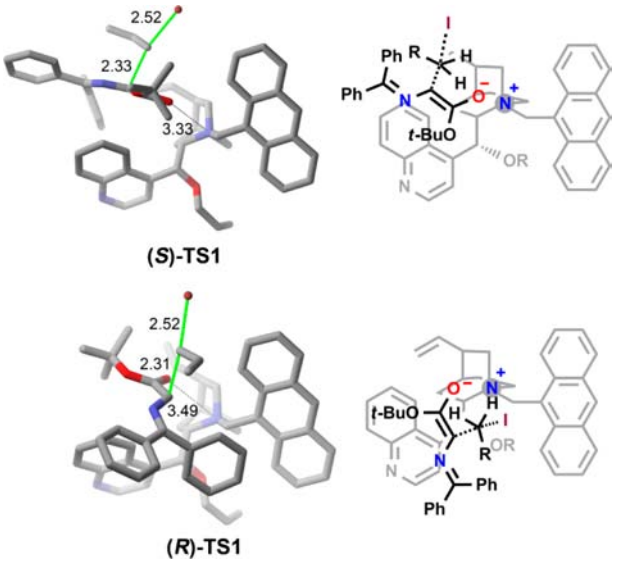

Figure 2. (left) Lowest energy enantiomeric allylation transition structures. (right) Lewis structure depictions of transition structures. Hydrogen atoms were removed for clarity.

The ensemble of low energy enolate−catalyst complexes suggests that a dynamic Curtin−Hammett model should apply to enantioselectivity.[11] Therefore we explored greater than 500 allylation transition structures leading to **(*S*)-3** and **(*R*)-3**. Again, this involved transition-structure searches done for both π-facial and oxy-anion approaches of the enolate to the three faces of catalyst **2** with all possible enolate and catalyst conformations.

The lowest energy allylation transition structures leading to **(*S*)-3** and **(*R*)-3** are shown in Figure 2. Both of the structures have similar partial C−C (2.3 Å) and partial C−Br (2.5 Å) bond lengths. In **(*S*)-TS1** the enolate α-carbon is pyramidalized by ∼10° while in **(*R*)-TS1** the α-carbon is slightly more pyramidalized to ∼15°. The $\Delta E^{\ddagger}_{soln}$ for **(*S*)-TS1** is 12.9 kcal/mol relative to **1**−**2** and allyl bromide. The $\Delta E^{\ddagger}_{soln}$ for **(*R*)-TS1** is 14.8 kcal/mol. The $\Delta\Delta E^{\ddagger}_{soln}$ of 1.9 kcal/mol corresponds to roughly 98% ee at −78 °C, which is in very good agreement with the results reported by Corey.[7]

In contrast to the ground-state complexes where the enolate interacts with catalyst **2** through a flat-π-facial mode, the lowest energy transition states located show that the enolate interacts with **2** via an oxy-anion interaction where the π-face is perpendicular to the ammonium tetrahedron face. This is the result of the pyramidalization and interaction with allyl bromide required at the α-enolate carbon in the transition states. We note that **(*S*)-TS1** is in agreement with the substrate−catalyst coordination complex proposed by Corey.[7] This mode of interaction was also proposed by Lygo and co-workers for their system.[17] The only major difference between **(*S*)-TS1** and Corey's model is the orientation of the quinoline group.[7,9]

Also different from the ground-state structures, there is a large energy difference between transition-state structures. There are only four transition structures that lead to **(*S*)-3** within 2 kcal/mol of **(*S*)-TS1**, and the second lowest energy transition structure that leads to **(*R*)-3** has a $\Delta E^{\ddagger}_{soln}$ of 16.8 kcal/mol and would not contribute to the formation of this enantiomer.

The structures of **(*S*)-TS1** and **(*R*)-TS1** highlight the dynamic Curtin−Hammett model because **(*S*)-TS1** does not arise from **1**−**2** and these transition states have different enolate−catalyst interaction conformations. Stated another way, selectivity does not arise from a single enolate−catalyst binding conformation where allylation occurs from either enolate π-face.

A stereoselectivity model also emerges from inspection of structures **(*S*)-TS1** and **(*R*)-TS1** that can be formulated within the context of the tetrahedron face model (Scheme 2a). Similar to the model proposed by Corey,[7] the rigid bicyclic core completely blocks one tetrahedron face and the anthracene group is rigid enough to block a second tetrahedron face. Transition structures with the enolate interacting with the ammonium center on the anthracenylmethyl side of catalyst **2** have energies that are greater than 15 kcal/mol higher than **(*S*)-TS1**, mostly due to the less favorable ground state coordination energy. This leaves only the pocket region between the arthracene and quinoline groups for interaction with the enolate.

Key to understanding the preference for electrophilic attack of the allyl bromide on the enolate *Re* face in **(*S*)-TS1** versus attack of the enolate *Si* face in **(*R*)-TS1** is the oxy-anion-quaternary ammonium interaction. In **(*S*)-TS1** the distance between the enolate O anion and the quaternary nitrogen is 3.33 Å while in **(*R*)-TS1** this same distance is

(17) Lygo, B.; Crosby, J.; Lowdon, T. R.; Peterson, J. A.; Wainwright, P. G. *Tetrahedron* **2001**, *57*, 2403.

3.49 Å. Also, in **(*S*)-TS1** the O anion is on average 0.1 Å closer to the quaternary ammonium N−CH bonds. These shorter interaction distances imply that the enolate−electrophile transition state geometry fits better into the pocket of catalyst **2** due to more favorable CH−π and π−π interactions in **(*S*)-TS1** compared to when the enolate-electrophile is flipped in **(*R*)-TS1**. Inspection of **(*S*)-TS1** bears this out. In **(*S*)-TS1** there are several optimal CH−π interactions. For example, the distance between a CH bond of the enolate phenyl group and the center of the quinoline aromatic ring is 2.34 Å. In addition to weak stabilizing interactions in **(*S*)-TS1**, the enolate O-*tert*-butyl group is oriented so that it is free from significant interaction with either the quinoline and anthracene groups. In contrast, in **(*R*)-TS1** the enolate phenyl groups are repulsed by the anthracene unit.

In conclusion, density functional theory was used to completely model enolate allylation of *tert*-butyl glycinate-benzophenone Schiff base **1** catalyzed by cinchonidinium catalyst **2**. This revealed that transition-state geometries involve oxy-anion (perpendicular π-face) interactions between the enolate and the quaternary ammonium. These calculations also suggest a dynamic Curtin−Hammett model with several low energy enolate−catlayst complexes that lead to a few highly selective transition states. Asymmetric stereoselectivity is the result of interactions that occur between the enolate-allyl transition-state geometry and the pocket region of catalyst CD **2**.

This study shows that quantum mechanical methods and transition-state analysis can now be used to model complex large phase-transfer catalysis systems and DFT will be useful for studying additional substrates and catalysts to elucidate general design considerations that may prove beneficial to further phase-transfer catalysis development.

Acknowledgment. We thank Brigham Young University (BYU) and the Fulton Supercomputing Lab. T.C.C. acknowledges the BYU Department of Chemistry and Biochemistry for support.

Supporting Information Available. Full ref 13, *xyz* coordinates, discussion of (*Z*) enolate. This material is available free of charge via the Internet at http://pubs.acs.org.

The authors declare no competing financial interest.